Cellular Dose Conversion Factors for α-Particle–Emitting Radionuclides of Interest in Radionuclide Therapy

Klaus A. Hamacher, Robert B. Den, Elana I. Den, and George Sgouros

Department of Medical Physics, Memorial Sloan-Kettering Cancer Center, New York, New York

α-Particle–emitting radionuclides are of increasing interest in radionuclide therapy. The decay scheme of α-emitting radionuclides typically includes a chain of unstable progeny. It is generally assumed that α-particle emission by the parent radionuclide will break the chemical bond with its carrier molecule and that the resulting daughter atom will no longer be associated with the carrier molecule. If the daughter is very short lived, it will not have enough time to be carried any significant distance from the site of parent decay and a cellular, absorbed dose estimate must consider the energy deposited by the daughter as well as the parent. Depending on the site of parent decay and the expected removal rate of daughter atoms from this site, the contribution of emissions from longer-lived daughters may also be warranted. In this study, dose conversion factors (DCFs) for cellular dimensions that incorporate the fate of daughter radionuclides were derived for ^{225}Ac, ^{213}Bi, ^{211}At, and ^{223}Ra, the α-particle–emitting radionuclides of interest in radionuclide therapy. **Methods:** The dose contribution of daughter radionuclides at the site of parent decay was made dependent on a cutoff time parameter, which was used to estimate the fraction of daughter decays expected at the site of parent decay. Previously tabulated S values (cell-surface to nucleus and cell-surface to cell) for each daughter in the decay scheme were scaled by this fraction and a sum over all daughters was performed to yield a cutoff time–dependent set of corresponding DCF values for each radionuclide. **Results:** DCF values for the absorbed dose to the nuclear or cellular volume from cell-surface decays are presented as a function of the cutoff time for 4 different cellular and nuclear dimensions. **Conclusion:** In contrast to the cellular S values that account only for parent decay, the DCF values provided in this study make it possible to easily include the contribution of daughter decays in cellular α-particle emitter dose calculations.

Key Words: α-particles; dosimetry; S values; dose conversion factors; ^{225}Ac; ^{211}At; ^{213}Bi; ^{223}Ra

J Nucl Med 2001; 42:1216–1221

Radionuclides that emit α-particles are of increasing interest in radionuclide therapy (*1,2*). Because the decay chain of several important α-particle emitters includes daughters that decay, which releases more α-particles, the cellular S value for the parent alone may not properly reflect the true α-particle energy deposition to a particular target per decay of the parent. The actual energy deposited will depend on the degree to which daughter decays contribute dose to the site of parent decay. This, in turn, will be influenced by the half-life of the daughter products and the rate at which they are removed from the site of parent decay. The latter will be related to the milieu within which the parent has decayed. If the half-life is very short compared with the removal or diffusion rate of the radionuclide, then the dose contribution from daughter decays should be included in cellular dose calculations.

In this study, we present a set of dose conversion factors (DCFs) that are analogous to cellular S values but extend this concept by including the cutoff time–dependent dose contribution of daughter decays at the site of parent decay. The cutoff time is thus introduced as a parameter that represents assumptions regarding the degree to which daughters should be included.

MATERIALS AND METHODS

Cellular S values for 4 α-particle emitters (^{225}Ac, ^{211}At, ^{213}Bi, and ^{223}Ra) and their progeny were obtained from the MIRD tabulation of cellular S values (*3*). S values for ^{213}Po, one of the elements in the decay chain of ^{213}Bi, are not tabulated and therefore needed to be calculated by spline interpolation of the monoenergetic α-particle S value tables. Similarly, S values for ^{207}Bi, one of the elements in the ^{211}At decay chain, which decays with electron capture or—albeit with very small probability—through positron decay, are not tabulated. These were calculated by spline interpolation as well. The contribution of daughter radionuclides to the absorbed dose at the site of parent decay was obtained by calculating the fraction of daughter decays, f, expected within a cutoff time parameter, τ_0.

The total number of daughter decays for a given initial radioactivity, A_0, is given by:

$$\int_0^\infty A_0 e^{-\lambda t} = \frac{1}{\lambda} A_0, \qquad \text{Eq. 1}$$

where $\lambda = [\ln(2)/T_{1/2}]$ and $T_{1/2} = $ the half-life of the radionuclide.

The number of decays occurring within τ_o is:

$$\int_0^{\tau_0} A_0 e^{-\lambda t} = \frac{1}{\lambda}(1 - e^{-\lambda\tau_0})A_0. \qquad \text{Eq. 2}$$

The ratio of Equations 1 and 2 gives the fraction of total decays, g, occurring within a cutoff time, τ_o:

$$g(\tau_0) = 1 - e^{-\lambda\tau_0} = 1 - e^{-\tau_0/\tau}, \qquad \text{Eq. 3}$$

where τ corresponds to the average lifetime of the radionuclide $(=1/\lambda)$.

Because the contributing fraction of daughter decays is dependent on the amount of daughter decays and the branching ratio (the percentage that decays into a specific daughter) of the radionuclide immediately preceding it, the actual fraction is the product of the calculated fraction, g_i, for daughter i, of the preceding radionuclide's calculated fraction, $g_{(i-1)}$, and of the branching ratio for production of daughter i, r_i:

$$f_i(\tau_0) = g_i(\tau_0)g_{(i-1)}(\tau_0)r_i. \qquad \text{Eq. 4}$$

These fractions, f_i, are then multiplied by the cellular S values, S_i, for each daughter i and summed to yield the final DCF,

$$\text{DCF}(\tau_0) = \sum_i f_i(\tau_0)S_i. \qquad \text{Eq. 5}$$

Equation 5 was used to generate graphs of DCFs as a function of τ_0 for [225]Ac, [213]Bi, [211]At, and [223]Ra for 4 different cellular dimensions.

RESULTS

Table 1 lists cellular S values for [213]Po, and Table 2 lists cellular S values for [207]Bi for various source–target combinations and increasing radii for cell (R_C) and nucleus (R_N). The possible source locations are cell, cell surface, cytoplasm, and nucleus. The targets are either cell (C) or nucleus (N). For example, S(N ← Cy) refers to the S value when the nucleus is the target and the activity is uniformly distributed in the cytoplasm (3). Figure 1 depicts the decay schemes of the 4 radionuclides studied (4). Figures 2 and 3 show the DCF plots for cell-surface to cell and cell-surface to nucleus for those radionuclides. With the exception of [213]Bi, DCF values at the shortest cutoff time (0.001 min) are comparable with the original cellular S value for a parent radionuclide. At the longest cut-off times (1,000 min), the DCF values reflect the sum of parent and all daughter S values.

Points of transition to higher DCF values reflect the inclusion of additional daughters as contributing to the

TABLE 1
Cellular S Values for [213]Po

R_C (µm)	R_N (µm)	S(C ← C) (Gy/Bq/s)	S(C ← CS) (Gy/Bq/s)	S(N ← N) (Gy/Bq/s)	S(N ← Cy) (Gy/Bq/s)	S(N ← CS) (Gy/Bq/s)
3	2	1.95E−01	1.30E−01	4.37E−01	1.50E−01	9.74E−02
3	1	1.95E−01	1.30E−01	1.74E+00	1.97E−01	8.97E−02
4	3	1.10E−01	7.36E−02	1.95E−01	8.02E−02	5.70E−02
4	2	1.10E−01	7.36E−02	4.37E−01	9.66E−02	5.23E−02
5	4	7.05E−02	4.72E−02	1.10E−01	4.99E−02	3.76E−02
5	3	7.05E−02	4.72E−02	1.95E−01	5.73E−02	3.45E−02
5	2	7.05E−02	4.72E−02	4.37E−01	6.75E−02	3.29E−02
6	5	4.91E−02	3.29E−02	7.05E−02	3.41E−02	2.67E−02
6	4	4.91E−02	3.29E−02	1.10E−01	3.79E−02	2.46E−02
6	3	4.91E−02	3.29E−02	1.95E−01	4.32E−02	2.34E−02
7	6	3.62E−02	2.43E−02	4.91E−02	2.48E−02	2.01E−02
7	5	3.62E−02	2.43E−02	7.05E−02	2.71E−02	1.85E−02
7	4	3.62E−02	2.43E−02	1.08E−01	3.01E−02	1.77E−02
7	3	3.62E−02	2.43E−02	1.95E−01	3.38E−02	1.70E−02
8	7	2.77E−02	1.86E−02	3.62E−02	1.89E−02	1.56E−02
8	6	2.77E−02	1.86E−02	4.91E−02	2.03E−02	1.45E−02
8	5	2.77E−02	1.86E−02	7.05E−02	2.22E−02	1.38E−02
8	4	2.77E−02	1.86E−02	1.10E−01	2.45E−02	1.33E−02
9	8	2.20E−02	1.48E−02	2.79E−02	1.49E−02	1.25E−02
9	7	2.20E−02	1.48E−02	3.62E−02	1.58E−02	1.16E−02
9	6	2.20E−02	1.48E−02	4.91E−02	1.71E−02	1.11E−02
9	5	2.20E−02	1.48E−02	7.05E−02	1.86E−02	1.07E−02
10	9	1.79E−02	1.79E−02	2.20E−02	1.21E−02	1.03E−02
10	8	1.79E−02	1.79E−02	2.77E−02	1.27E−02	9.60E−03
10	7	1.79E−02	1.79E−02	3.62E−02	1.35E−02	9.15E−03
10	6	1.79E−02	1.79E−02	4.91E−02	1.46E−02	8.82E−03
10	5	1.79E−02	1.79E−02	7.05E−02	1.57E−02	8.60E−03

R_C = cellular radius; R_N = nuclear radius; C = cell volume; CS = cell surface; N = nucleus; Cy = cytoplasm; S(X ← Y) = S factor for X target and Y source.

TABLE 2
Cellular S Values for [207]Bi

R_C (μm)	R_N (μm)	S(C ← C) (Gy/Bq/s)	S(C ← CS) (Gy/Bq/s)	S(N ← N) (Gy/Bq/s)	S(N ← Cy) (Gy/Bq/s)	S(N ← CS) (Gy/Bq/s)
3	2	2.55E−03	1.82E−03	5.35E−03	2.03E−03	1.41E−03
3	1	2.55E−03	1.82E−03	2.03E−02	2.58E−03	1.32E−03
4	3	1.57E−03	1.10E−03	2.55E−03	1.26E−03	9.83E−04
4	2	1.57E−03	1.10E−03	5.35E−03	1.41E−03	9.34E−04
5	4	1.02E−03	6.69E−04	1.57E−03	7.87E−04	6.01E−04
5	3	1.02E−03	6.69E−04	2.55E−03	9.62E−04	6.29E−04
5	2	1.02E−03	6.69E−04	5.35E−03	1.11E−03	7.23E−04
6	5	6.87E−04	4.29E−04	1.02E−03	4.87E−04	3.73E−04
6	4	6.87E−04	4.29E−04	1.57E−03	5.97E−04	3.69E−04
6	3	6.87E−04	4.29E−04	2.55E−03	7.36E−04	3.85E−04
7	6	4.80E−04	2.89E−04	6.87E−04	3.16E−04	2.44E−04
7	5	4.80E−04	2.89E−04	1.02E−03	3.72E−04	2.27E−04
7	4	4.80E−04	2.89E−04	1.57E−03	4.56E−04	2.15E−04
7	3	4.80E−04	2.89E−04	2.55E−03	5.56E−04	1.99E−04
8	7	3.47E−04	2.03E−04	4.80E−04	2.15E−04	1.67E−04
8	6	3.47E−04	2.03E−04	6.87E−04	2.44E−04	1.48E−04
8	5	3.47E−04	2.03E−04	1.02E−03	2.86E−04	1.31E−04
8	4	3.47E−04	2.03E−04	1.57E−03	3.42E−04	1.08E−04
9	8	2.58E−04	1.49E−04	3.47E−04	1.53E−04	1.19E−04
9	7	2.58E−04	1.49E−04	4.80E−04	1.68E−04	1.02E−04
9	6	2.58E−04	1.49E−04	6.87E−04	1.89E−04	8.59E−05
9	5	2.58E−04	1.49E−04	1.02E−03	2.17E−04	6.55E−05
10	9	1.97E−04	1.12E−04	2.58E−04	1.12E−04	8.77E−05
10	8	1.97E−04	1.12E−04	3.47E−04	1.20E−04	7.32E−05
10	7	1.97E−04	1.12E−04	4.80E−04	1.31E−04	5.93E−05
10	6	1.97E−04	1.12E−04	6.87E−04	1.45E−04	4.30E−05
10	5	1.97E−04	1.12E−04	1.02E−03	1.63E−04	2.30E−05

R_C = cellular radius; R_N = nuclear radius; C = cell volume; CS = cell surface; N = nucleus; Cy = cytoplasm; S(X ← Y) = S factor for X target and Y source.
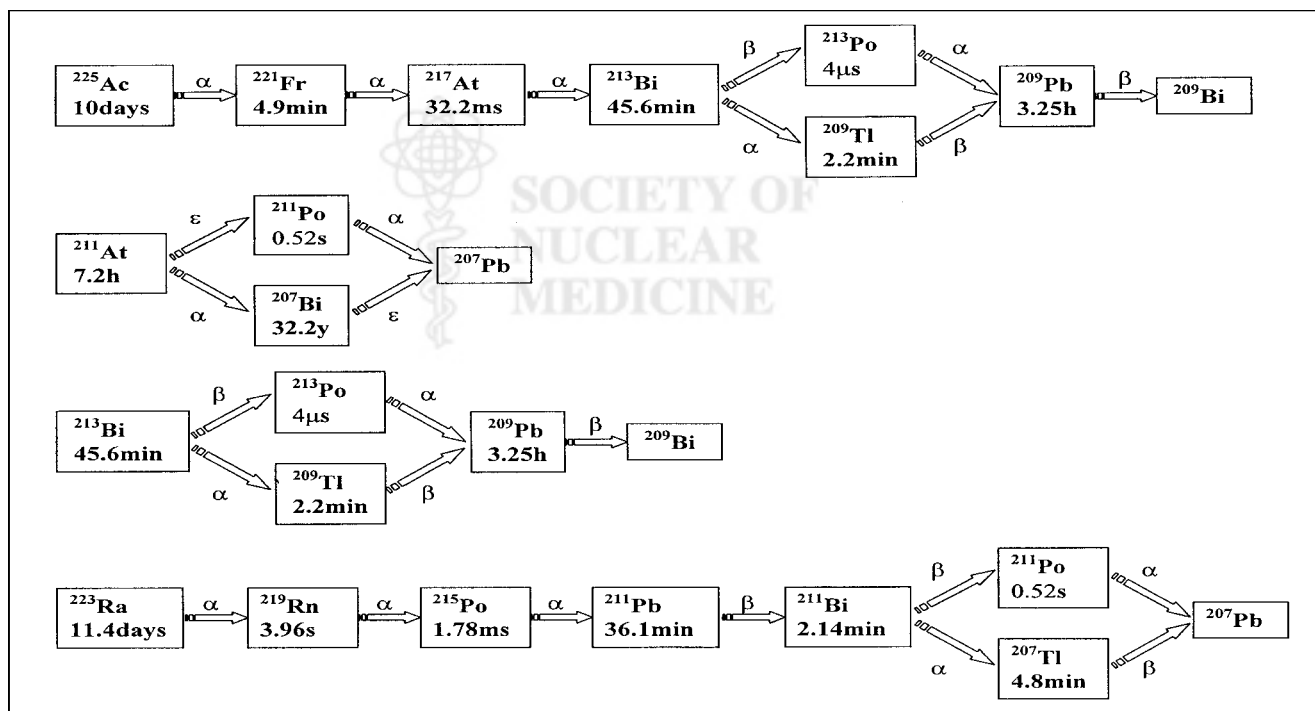
FIGURE 1. Decay schemes for [225]Ac, [211]At, [213]Bi, and [223]Ra.
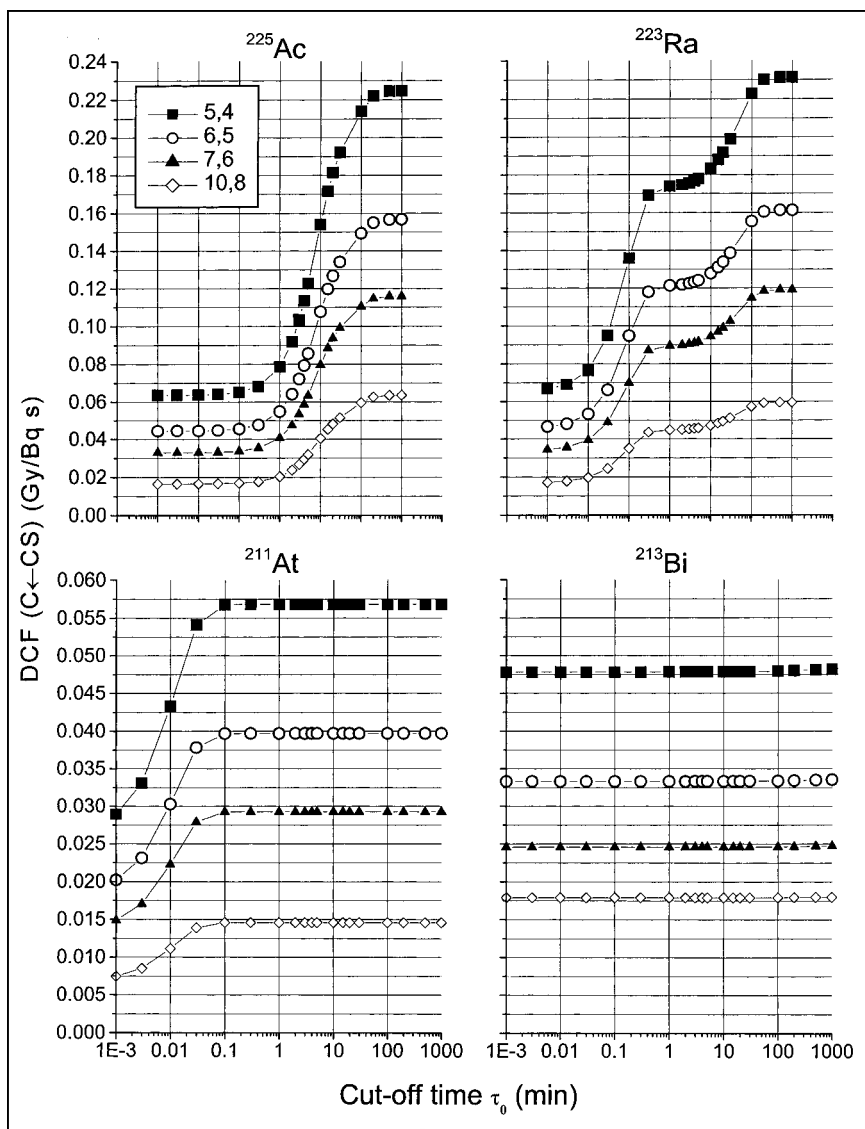
FIGURE 2. DCF values vs. τ_0 for (C ← CS) where CS represents cell surface. Plots for several different cellular dimensions are shown and denoted by (R_C, R_N), representing radius of cell and of nucleus, respectively.

absorbed dose at the site of parent decay. In the ^{223}Ra graph (Fig. 2), a plateau is present from 0 min to approximately 0.01 min because only the parent contributes. From $\tau_0 = 0.01$ min through $\tau_0 = 0.3$ min, an increase in the DCF can be seen that is caused by the progressive retention of ^{219}Rn ($\tau = 0.1$ min) and ^{215}Po ($\tau = 4 \times 10^{-5}$ min) at the site of parent decay. Because ^{215}Po has an average lifetime shorter than that of ^{219}Rn, the fraction of ^{215}Po that is removed from the ^{219}Rn decay site is smaller than the fraction of ^{219}Rn that is removed from the ^{223}Ra decay site. Thus, both will always contribute together to the DCF. The plateau present from $\tau_0 = 0.3$ min through $\tau_0 = 10$ min represents cutoff times at which the emissions from subsequent daughters may be ignored. The next increase, from $\tau_0 = 10$ min through $\tau_0 = 100$ min, represents the inclusion of ^{211}Pb ($\tau = 52$ min) and all subsequent daughter radionuclides at the site of parent decay. The last plateau, from 100 min to 1,000 min, corresponds to the maximum DCF value in which all daughters are included. In the plot for ^{213}Bi (Fig. 2), the S value

contribution of the β-emitter, ^{209}Pb ($\tau = 281$ min), although small relative to α-particle S values, may be seen as a slight increase between 100 min and 1,000 min.

DISCUSSION

The decay scheme of α-particle–emitting radionuclides typically includes a chain of unstable progeny. It is generally assumed that α-particle emission by the parent radionuclide will break the chemical bond with its carrier molecule and that the resulting daughter atom will no longer be associated with the carrier molecule. If the daughter is very short lived (e.g., ^{213}Po with a 4.2-μs half-life), then it will not have enough time to move any significant distance from the site of parent decay and an absorbed dose estimate must consider energy deposited by the daughter as well as by the parent.

Drawing on recently published cellular S values and incorporating the considerations described above, we have

FIGURE 3. DCF values vs. τ_0 for (N ← CS) where CS represents cell surface. Plots for several different cellular dimensions are shown and denoted by (R_C, R_N), representing radius of cell and of nucleus, respectively.
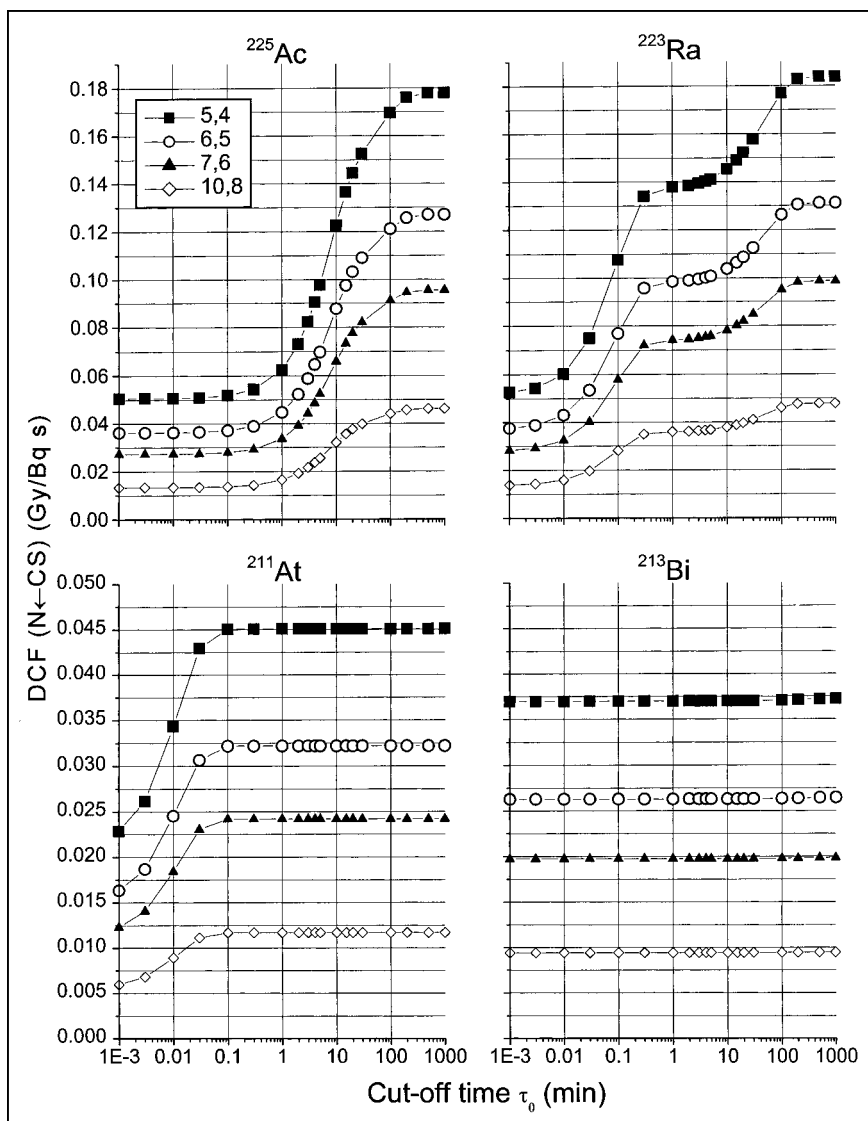
derived DCFs for α-particle–emitting radionuclides that either have already been used clinically, such as [213]Bi and [211]At, (5,6) or are considered to be promising candidates for clinical use, such as [225]Ac and [223]Ra (7,8).

Using Figures 2 and 3, biologic and kinetic considerations regarding the site of parent decay and possible fate of daughters may easily be incorporated into cellular absorbed dose calculations. Because blood convection will lead to a more rapid loss of daughter radionuclides from the site of parent decay than would tumor interstitium diffusion, the likelihood that daughters generated within the circulation will contribute significantly to the dose at the site of parent decay is considerably less than if the daughters were generated within the interstitium. By selecting appropriate cutoff times in Figures 2 and 3, different levels of daughter contribution may be chosen to match the milieu in which the parent radionuclide decays. In general, DCFs for parent decays in circulation are best approximated by the leftmost portions of the plots, where only the parent is included. In

the tumor interstitium, longer cutoff times may be appropriate and the middle portions of the plots would apply. The rightmost portions of the plots should be used to obtain DCF values in situations in which all daughters are expected to remain at the site of parent decay.

CONCLUSION

The extent to which daughter products remain at the site of parent decay will greatly influence the potential efficacy, toxicity, and clinical utility of α-particle–emitting radionuclides with decay schemes that include α-particle–emitting daughters. The figures presented in this article facilitate the use of different assumptions regarding daughter radionuclide retention at the site of parent decay.

ACKNOWLEDGMENTS

REFERENCES

1. Bigler RE, Zanzonico PB, Cosma M, Sgouros G. Adjuvant radioimmunotherapy for micrometastases: a strategy for cancer cure. In: Srivastava SC, ed. *Radiolabeled Antibodies for Imaging and Therapy: Proceedings of NATO Advanced Study Institute*. New York, NY: Plenum Press; 1988:409–429.

2. McDevitt MR, Sgouros G, Finn RD, et al. Radioimmunotherapy with alpha-emitting nuclides. *Eur J Nucl Med.* 1999;25:1341–1351.

3. Goddu SM, Howell RW, Bouchet LG, Bolch WE, Rao DV. *MIRD Cellular S Values*. Reston, VA: Society of Nuclear Medicine; 1997.

4. Browne E, Firestone RB. *Table of Radioactive Isotopes*. Shirley VS, ed. New York, NY: John Wiley & Sons; 1986.

5. Jurcic JG, McDevitt MR, Sgouros G, et al. Targeted alpha-particle therapy for myeloid leukemias: a phase I trial of bismuth-213-HuM195 (anti-CD33) [abstract]. *Blood.* 1997;90(suppl):504a.

6. Zalutsky MR, Bigner DD. Radioimmunotherapy with alpha particle-emitting radioimmunoconjugates. *Acta Oncol.* 1996;35:373–379.

7. Geerlings MW, Kaspersen FM, Apostolidis C, van der Hout R. The feasibility of ^{225}Ac as a source of alpha-particles in radioimmunotherapy. *Nucl Med Commun.* 1993;14:121–125.

8. Fisher DR, Sgouros G. *Dosimetry of Radium-223 and Progeny: Proceedings of the 6th International Radiopharmaceutical Dosimetry Symposium*. Oak Ridge, TN: U.S. Department of Energy and Oak Ridge Associated Universities; 1996.